the symmetry of the $[Cu(CO_3)_2]^{2-}$ unit is much higher.[7] A consideration of the possible exchange pathways using orbital symmetry relationships and the carbonate molecular orbitals indicates that both antiferromagnetic and ferromagnetic pathways are possible. Obviously the latter dominate in this case. This will be considered in more detail in due course.[13] Apart from $K_2Cu(CO_3)_2$ copper(II) oxydiacetate is the only other system where superexchange via a similar bridging unit results in ferromagnetic intralayer exchange ($J = 4.66$ cm^{-1}).[14] Here the CO_2^- group bridges adjacent coppers in a rather puckered fashion and the σ mechanism was thought to be mainly responsible for the observed interaction.

One of the more difficult problems in these layered materials is the question of exactly why some order ferromagnetically and others order antiferromagnetically. For example the layers in K_2CuF_4 and $[CH_3NH_3]_2CuCl_4$ couple ferromagnetically whereas in the other $CuCl_4^{2-}$ derivatives they couple antiferromagnetically. Hatfield and co-workers have tried to identify some of the features which determine the type of three-dimensional ordering which results in these types of compounds.[14] In $Na_2Cu(CO_3)_2$ this feature is probably easier to understand because of the detailed nature of the structure. Each copper ion in a layer has an identical copper ion as its immediate neighbor in the layers above and below. This may then encourage some sort of direct exchange between the copper ions in adjacent layers or even a superexchange via the interleaved sodium ions and so an antiferromagnetic interlayer coupling.

Acknowledgment. Financial support from the Australian Research Grants Committee and a Postgraduate Research Award (to N.T.M.) are gratefully acknowledged.

Registry No. $Na_2Cu(CO_3)_2$, 37224-64-9; $Na_2Cu(CO_3)_2$ (salt), 37224-64-9.

---

[13] Gregson, A. K.; Moxon, N. T., to be submitted for publication.

[14] Corvan, P. J.; Estes, W. E.; Weller, R. R.; Hatfield, W. E. *Inorg. Chem.* **1980**, *19*, 1297.

Contribution from the Department of Physical and Inorganic Chemistry,
University of New England, Armidale, N.S.W., Australia 2351

Quantitative Description of the Magnetic Properties and Proton Isotropic Shifts of Hemichrome Salts (Derivatives of Iron(III) Octaethylporphyrin Complexes): The Presence of a Spin Equilibrium

ANTHONY K. GREGSON

Received March 13, 1980

A quantitative interpretation of the temperature-dependent magnetic and NMR properties of a series of $Fe(OEP)X_2ClO_4$ derivatives is given by using the quantum mechanical spin-mixed model (OEP = octaethylporphyrin, X = heterocyclic base). A small temperature variation in the ligand-field parameters ($\sim$1%) is necessary to account for both the magnetic and NMR data. In the quantum mechanical spin-mixed model limiting high-temperature magnetic moments of between 4.0 and 4.5 μ_B are not necessarily an indication of a spin quartet state.

Introduction

In view of the recent articles on the possibility of quantum mechanical spin-mixed ground states for several iron-containing proteins[1] and even (octaethylporphyrinato)iron(III) perchlorate, $Fe(OEP)ClO_4$,[2] we are prompted to report in detail some calculations made several years ago[3] on the rather unusual magnetic and NMR properties of the series $Fe(OEP)X_2ClO_4$ (X = substituted heterocyclic base (Figure 1)). Our description is tentative and probably not unique although it does offer a tenable phenomenological *quantitative* explanation which is consistent with most of the available experimental data.

The magnetic properties of the $Fe(OEP)X_2ClO_4$ derivatives[3b,4] (summarized in Figure 2) are unlike those of typical high-spin ($S = {}^5/_2$) or low-spin ($S = {}^1/_2$) ferric heme proteins. In some respects they resemble more the properties of several of the ferricytochromes *c′* where a quantum mechanical admixture of the intermediate-spin state ($S = {}^3/_2$) with the $S = {}^5/_2$ state was able to reproduce the experimental data to a very good approximation.[1] The data shown in Figure 2 are different from the ferricytochromes *c′* in that there appears to be an apparent (see later) equilibrium between the intermediate $S = {}^3/_2$ state and the low-spin $S = {}^1/_2$ state.

The very large changes in magnetic moment over such a small temperature range (4.22–2.7 μ_B over 120 K in the extreme case) are most unusual and probably indicate a changing spin state and/or some type of spin-equilibrium situation. This can be looked at in several ways. The first considers the equilibrium to consist of simple thermal mixtures over noninteracting $S = {}^5/_2$, ${}^3/_2$, and ${}^1/_2$ levels on one molecule; the second would be a similar equilibrium but over different molecules. A combination of these was the first to be proposed and can be often account for the magnetic data of iron(III) materials possessing spin-equilibrium properties.[5] The third possibility involves a quantum mechanical mixture, first introduced by Harris,[6] which allows spin–orbit coupling to mix all the levels to give a thermal average over a single molecule.[1] The real situation may even be different quantum mechanical mixtures over different molecules although this would be too difficult for a quantitative description. The observed magnetic properties of the first two models would be similar except if the populations of different molecules with different ground states did not follow a Boltzmann distribution. These cooperative spin transitions are known[7] but probably do not exist in this case because the solution (from NMR measurements) and solid-state magnetic data are very similar.[3b] This latter observation also eliminates two further situations: (i) an equilibrium between chemically different species in solution

---

[1] (a) Maltempo, M. M. *J. Chem. Phys.* **1974**, *61*, 2540. (b) Maltempo, M. M.; Moss, T. H. *Q. Rev. Biophys.* **1976**, *9*, 181.

[2] Dolphin, D. H.; Sams, J. R.; Tsui, T. B. *Inorg. Chem.* **1977**, *16*, 711.

[3] (a) First presented at a Royal Australian Chemical Institute symposium on "Magnetism and Transition Metal Compounds", Monash University, Melbourne, Australia, Nov 1975. (b) Hill, H. A. O.; Skyte, P. D.; Buchler, J. W.; Lueken, H.; Tonn, M.; Gregson, A. K.; Pellizer, G. *J. Chem. Soc., Chem. Commun.* **1979**, 151.

[4] Skyte, P. D. D.Phil. Thesis, University of Oxford, 1976.

[5] Martin, R. L.; White, A. H. *Transition Met. Chem.* **1968**, *4*, 113.

[6] Harris, G. *Theor. Chim. Acta (Berlin)* **1968**, *10*, 119, 155.

[7] For example see: Konig, E.; Ritter, G.; Kanellakopulos, B. *J. Phys. C* **1974**, *7*, 2681.

0020-1669/81/1320-0081$01.00/0 © 1981 American Chemical Society

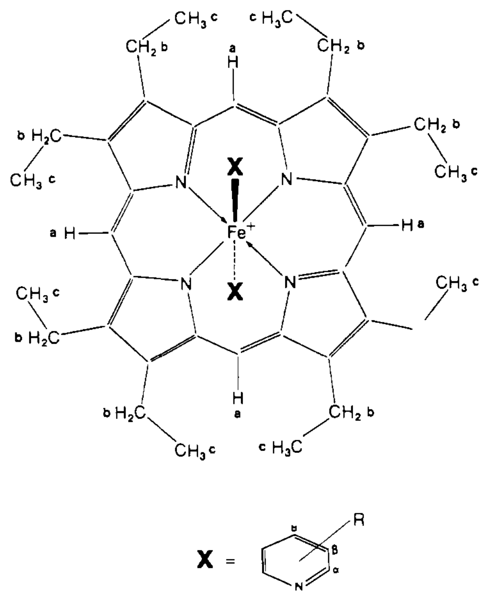

Figure 1. Structure of the $Fe(OEP)X_2^+$ complex with assignment nomenclature.

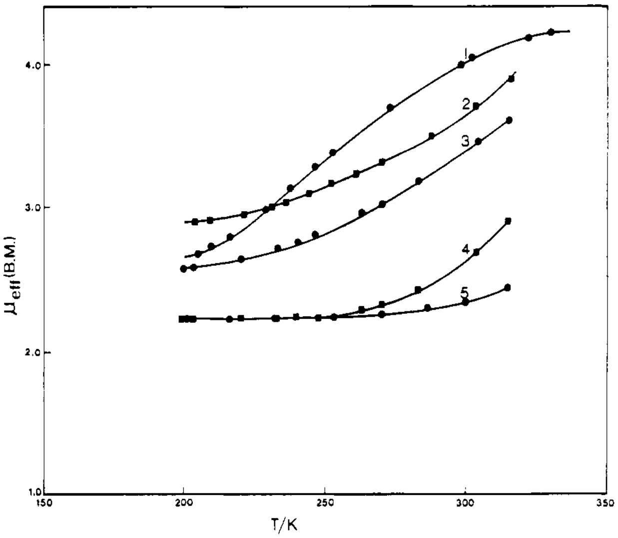

Figure 2. Summary of the solution magnetic moments (NMR method and taken from ref 4) of several substituted $Fe(OEP)X_2ClO_4$ compounds where X = 3-chloropyridine (1), 4-acetylpyridine (2), 3-acetylpyridine (3), pyridine (4), and *N*-methylimidazole (5). Solid lines are a guide to the eye.

and (ii) cooperative phenomena in the solid.

The associated isotropic NMR shifts are also atypical of normal high- or low-spin iron(III) compounds and are obviously intimately connected with the unusual spin state of the metal ion. A quantitative explanation of the magnetic and NMR behavior of these $Fe(OEP)X_2ClO_4$ derivatives is attempted below.

Experimental Section

All the physical measurements were made by using equipment and procedures which have been described previously.[8] The solution magnetic moments were determined[4] by using standard NMR techniques[9] and are summarized in Figure 2. The solid-state magnetic moments of these compounds are very similar to those shown in Figure 2.[3b]

The magnetic properties were calculated by using the computer programs VVLH and VVLE. These allow the magnetic properties to be calculated as a function of temperature, any of the ligand-field parameters, and the applied magnetic-field strength. This is accomplished by calculating $\partial E/\partial H$ directly and then by using the Van Vleck equation and has been described recently.[10] The explicit inclusion of the applied magnetic field takes account of the effects of magnetic saturation (in this case they may not be insignificant when the magnetic field of the NMR instrument is considered, 14 100 Oe) and also allows the calculation of the required parameters in the isotropic shift problem in paramagnetic molecules.

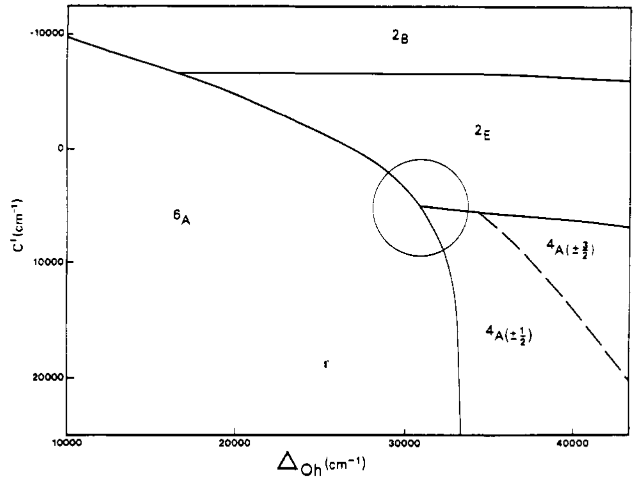

Figure 3. Regions of parameter space (Δ_{Oh} and C') defining the different ground states for the d^5 ferric ion, calculated with $f = 1.0$, $B = 1100\ cm^{-1}$, $C = 3750\ cm^{-1}$, and $\zeta = 420\ cm^{-1}$. The circle indicates the postulated region of interest for many ferric heme compounds.

The Magnetic Model

In cubic symmetry there are two possible ground states for the iron(III) ion, namely, the high-spin $^6A_{1g}$ state or the low-spin $^2T_{2g}$ state. In strongly tetragonal symmetry (assumed to be D_4) there are two possible low-spin ground states arising from the splitting of the $^2T_{2g}$ state into ^2E and $^2B_2$. An intermediate $S = {}^3/_2$ state ($^4A_2$) can also, in certain circumstances, become the ground state.

Recently the magnetic properties of the d^5 configuration have been considered[11] by taking account of the $^6A_{1g}$, $^4T_{1g}$, and $^2T_{2g}$ cubic field states which, in a strong tetragonal field, gives rise to all the possible ground states. This was based on the work of Harris[6] and included spin–orbit coupling (ζ) between all states and full parameterization of the ligand field in terms of the Racah parameters *B* and *C* and three others: Δ_{Oh}, C', and *f*. Δ_{Oh} is the octahedral crystal-field parameter and in the present model is interpreted as the average effect of all six ligands in the given complex. C' is a measure of the axial components of the ligand field and goes to zero in the limit of cubic symmetry. *f* is a constant relating the relative magnitude of the t_{2g} and e_g tetragonal splittings and is normally given the value 1.0.[6] In all the calculations the free-ion values of ζ, *B*, and *C* have been used (420, 1100, and 3750 cm^{-1}, respectively), thus reducing the number of varying parameters.

A consideration of Figure 3 shows the regions of parameter space giving rise to the various possible ground states in the d^5 electronic configuration. The states shown are the only ones which can have a significant effect on the ground-state magnetic properties of an ion with this particular configuration. There is however one possible situation where this is not strictly true and occurs when the quartet spin state ($^4A_2$) is lowest in energy.[12] An excited ^4E state from a higher lying $^4T_1$ level can play a major role in determining the zero-field splitting

---

(8) Hill, H. A. O.; Morallee, K. G. *J. Am. Chem. Soc.* **1972**, *94*, 731.

(9) Evans, D. F. *J. Chem. Soc.* **1959**, 2003.

(10) Gregson, A. K. *Aust. J. Chem.*, in press.

(11) (a) Gregson, A. K. Ph.D. Thesis, University of Melbourne, 1971. (b) Barraclough, C. G.; Gregson, A. K.; Mitra, S. *J. Chem. Phys.* **1974**, *60*, 962.

(12) Marathe, V. R.; Mitra, S. *Ind. J. Pure Appl. Phys.* **1976**, *14*, 893.

Table I. Magnetic Parameters for Several $Fe(OEP)X_2ClO_4$ Derivatives

derivative	T/K	$\mu_{\parallel}/\mu_B$[a]	$\mu_{\perp}/\mu_B$[a]	$\bar{\mu}/\mu_B$[a]	$\bar{\mu}_{exptl}/\mu_B$[b]	Δ_{Oh}/cm^{-1}	C'/cm^{-1}
3-chloropyridine	320	4.36	4.14	4.22	4.20	31 950	4425
	260	3.90	3.18	3.44	3.50	32 000	4405
	200	3.57	2.09	2.68	2.65	32 055	4395
4-acetylpyridine	320	4.16	3.76	3.89	3.89	31 970	4400
	260	3.79	2.94	3.25	3.23	32 000	4380
	200	3.65	2.37	2.86	2.86	32 000	4380
3-acetylpyridine	320	4.04	3.53	3.70	3.70	32 000	4400
	260	3.69	2.67	3.05	2.95	32 000	4350
	200	3.57	2.13	2.69	2.60	32 000	4350
pyridine	320	3.66	2.76	3.09	3.10	32 000	4300
	260	3.40	1.93	2.52	2.40	32 050	4250
	200	3.39	1.61	2.35	2.30	32 050	4250
N-methylimidazole	320	3.24	1.91	2.43	2.43	32 000	4000
	260	3.27	1.74	2.36	2.30	32 000	4000
	200	3.29	1.57	2.29	2.25	32 000	4000

[a] Calculated by using the accompanying values of Δ_{Oh} and C'; values for the other parameters are described in the text. [b] From ref 3b and 4.

properties of the $^4A_2$ state, but in the present situation, with the dominating $^6A_1$ state so near in energy, this interesting feature of the d^5 electronic configuration should not concern us here.

Comparison of Theory with Experiment

(i) Noninteracting Model. With magnetic moments ranging from 2.2 to ~4.2 μ_B the simplest starting point would be a consideration of a noninteracting quartet–doublet equilibrium involving the $^4A_2$ and $^2T_2$ states. This is easily achieved on the Harris model by removing all the spin–orbit coupling matrix elements connecting the quartet and doublet states and placing the $^6A_1$ state at a very high energy and thereby making no contribution to the magnetic state of the ion. The parameters describing the $^2T_2$ ground state are easily deduced from a knowledge of the limiting magnetic moment of ~2.2 μ_B for the *N*-methylimidazole and pyridine derivatives. This value of μ_{eff} is compatible with an axial-field splitting of ~2000 cm^{-1}; the corresponding calculated g values are then $g_{\parallel} = 3.9$ and $g_{\perp} = 0.3$ which are approximately those reported for the Fe^{III}(protoporphyrin IX)$(py)_2Cl$ complex.[8] This is also consistent with the large quadrupole splitting of the $^2T_2$ species observed in the Mössbauer spectrum of $Fe(OEP)(py)_2ClO_4$.[13]

However problems arise when a pure $^4A_2$ level is used as the excited spin-state species. The average magnetic moment is not nearly high enough, 4.0 μ_B being a near upper limit, even considering the splitting of the parental $^4T_1$ state to be small or zero. So that this difficulty can be overcome in the high-moment end of the observed range of μ_{eff} values the $^6A_1$ level can be lowered, and indeed when placed approximately 800 cm^{-1} above the formal $^4T_1$ state, the correct high-temperature magnitude of μ_{eff} can be obtained, namely, ~4.2 μ_B for the 3-chloropyridine derivative.

Given that the two extremes in magnetic moment can now be predicted (i.e., 2.2 and 4.2 μ_B) there are still major difficulties with this description because unlimited parameter juggling cannot reproduce the large magnetic moment change over the small temperature range (320–200 K). As well, the present set of experimental observations, even in a very crude sense, can only be consistent with a set of ligand field parameters close to the "triple point" of Figure 3, i.e., very close to the region where $^6A_1$, $^4A_2$, and ^2E are approximately equienergetic. If this is the case, then the quantum mechanical spin-mixed model *must* be more appropriate because, if the three states in question are so close to each other in energy, the neglect of spin–orbit mixing between them is simply not realistic. Accordingly we now turn to an examination of the complete Harris model including spin–orbit coupling and all the relevant crystal field perturbations.

(ii) Interacting Model. The 3-chloropyridine derivative is chosen first because it has the highest magnetic moment at 320 K (4.22 μ_B) and also the largest temperature variation, falling to 2.7 μ_B by 205 K. With the free-ion values for ζ, B, and C mentioned above and 31 950 and 4450 cm^{-1} for Δ_{Oh} and C', respectively, the correct value of ~4.22 μ_B is predicted at 320 K. The latter two values were arrived at by plotting the change in magnetic moment as a function of Δ_{Oh} and C' at 320 K and selecting the appropriate combination—a somewhat arbitrary procedure but nonetheless satisfactory for the present purpose. However similar difficulties to the noninteracting quartet–doublet equilibrium were experienced in that the large drop in magnetic moment (~1.5 μ_B) over the temperature range 320–200 K just cannot be reproduced theoretically. This difficulty applies in varying degrees to all the compounds whose magnetic properties were measured and, as well, to several of the temperature-dependent isotropic NMR shifts (see below).

A way out of this dilemma is not easy as both the thermal and quantum mechanical mixing models are both unable to produce the desired magnetic moment variation with temperature, even with large scale variation of all possible parameters. The effect of a substantial zero-field splitting on the quartet and sextet states was then investigated. Splittings of more than 100 cm^{-1} were tried (not unreasonable as, for example, in the related manganese(II) and iron(II) phthalocyanine derivatives the zero-field splitting is 40[11] and 60[14] cm^{-1}, respectively). Although this made a small difference, and in the correct direction, the predicted moments were still a long way from the experimental data. As a final resort temperature-dependent ligand-field parameters were investigated. At first sight this is most unsatisfactory, but on closer examination it may be a plausible explanation, the justification of which will be attempted below.

Taking the highest magnetic moment first, we find that at 320 K the measured value can be reproduced with Δ_{Oh} = 31 950 and C' = 4425 cm^{-1}, respectively. Values of 32 000 and 4405 cm^{-1}, respectively, at 260 K and 32 055 and 4395 cm^{-1}, respectively, at 200 K then lead to quantitative agreement at the three selected temperatures. This is plotted in Figure 4 to clarify the magnetic moment variation with temperature for the three sets of parameters. If we then assume smooth variations in Δ_{Oh} from 31 950 to 32 055 cm^{-1} and in C' from 4425 to 4395 cm^{-1}, respectively, the magnetic properties of the (3-Cl-py)(OEP) derivative are accounted for. Similar variations in the ligand-field parameters can reproduce all the measured magnetic moments; the values are listed in

---

(13) Hill, H. A. O.; Skyte, P.; Dale, B., unpublished results.

(14) Barraclough, C. G.; Martin, R. L.; Mitra, S.; Sherwood, R. C. *J. Chem. Phys.* **1970**, *53*, 1643.

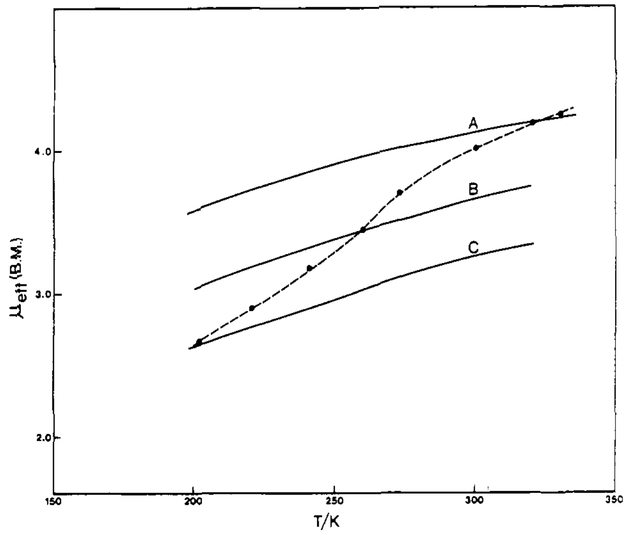

Figure 4. Theoretical and experimental magnetic moments for Fe(OEP)(3-Cl-py)$_2$ClO$_4$. The solid lines have been calculated with (A) Δ_{Oh} = 31 950 and C' = 4425 cm^{-1}, (B) Δ_{Oh} = 32 000 and C' = 4405 cm^{-1}, and (C) Δ_{Oh} = 32 055 and C' = 4395 cm^{-1}. The experimental data are shown by ●.

Table I. It must be appreciated that these may not be unique, and other combinations, even within the present model, could probably reproduce the experimental data just as well.

The changing parameters in Table I mean that in lowering the temperature from 320 to 200 K the ligand field around the metal ion is becoming more cubic in the sense that the difference between in-plane and axial-field strengths is slightly smaller because Δ_{Oh} is increasing and the tetragonality parameter is becoming smaller. This could quite easily correspond to the iron atom moving relative to the plane of the heme-type ring. This is an attractive possibility because it is now recognized that conformational changes involving the position of the iron atom along the z axis with respect to the heme plane are probably crucial in determining the properties of the high-, low-, and intermediate-spin iron proteins. (Even if the iron atom did not formally move, it is known[15] that an equivalent approach is to include a vibrational partition parameter.) It has also been suggested that in the ferricytochromes c' the several different intermediate values of magnetic moment arise from different spin-state admixtures which in turn depend on the different distances the iron atom may be placed from the heme plane, and indeed the sense and direction of the resulting orbital energies obtained by Maltempo[1] are very similar to those obtained in the present work. If the magnetic properties are then dependent on such sensitive factors, the fact that the position of the iron atom out of the heme plane being only slightly temperature dependent appears not unreasonable. The magnitude of the changes is also quite small, being only ~3% for Δ_{Oh} and ~1% for C'. However even these quite small changes produce significant changes in the magnetic state of the iron atom because the spin-mixed region ($^6A_1$, $^4A_2$, and ^2E in D_4 symmetry) appears to control the overall properties of the metal ion in question.

At this stage it is useful to look in a little detail at the actual composition of the ground and excited states of the iron atom in these OEP derivatives. There are two distinctly different types of state (classified in the D_4 double group) for the d^5 ion in this environment, namely, E′ and E″. In all cases the ^4E state always occurs at relatively high energies (>10 000 cm^{-1} above the ground state), so it will be neglected in the following discussion. The E″ state then contains the components $^6A_1$ ($\pm^5/_2$), $^6A_1$ ($\mp^3/_2$), $^4A_2$ ($\pm^3/_2$), ^2E ($\pm^1/_2$, ∓1), and $^2B_2$ ($\pm^1/_2$) while E′ states are composed of $^6A_1$ ($\pm^1/_2$), $^4A_2$ ($\pm^1/_2$), and ^2E ($\pm^1/_2$, ±1) components. The ground state is always E″ and dominated by ^2E character. Not surprisingly, this increases from 77% (the $^6A_1$ ($^3/_2$), $^4A_2$ ($^3/_2$), $^2B_2$ ($^1/_2$), and $^6A_1$ ($^5/_2$) components contribute approximately 10, 8, 3, and 1%, respectively) for the 3-chloropyridine derivative (4.22 μ_B at 320 K) to 86% for the N-methylimidazole derivative (2.4 μ_B at 320 K). As well the changing ligand-field parameters with temperature lead to increased ^2E character in the ground state, mainly at the expense of the $^6A_1$ ($^3/_2$) component. The excited states are shown in Figure 5, and apart from the two that are mainly comprised of $^6A_1$ ($^1/_2$) and ^2E ($\pm^1/_2$, ±1) they are all predominately single component levels and are so labeled in Figure 5. The two E′ states composed mainly of $^6A_1$ ($^1/_2$) and ^2E ($\pm^1/_2$, ±1) have varying composition. For example the lower one (first excited state) comprises 85% $^6A_1$ and 65% ^2E for a magnetic moment of 4.2 μ_B whereas 96% ^2E character is predicted for a magnetic moment of 2.4 μ_B, the amount of ^4A ($^1/_2$) remaining approximately constant. The reverse occurs for the second E′ state while the third E′ state always remains predominately $^1A_2$ ($^1/_2$).

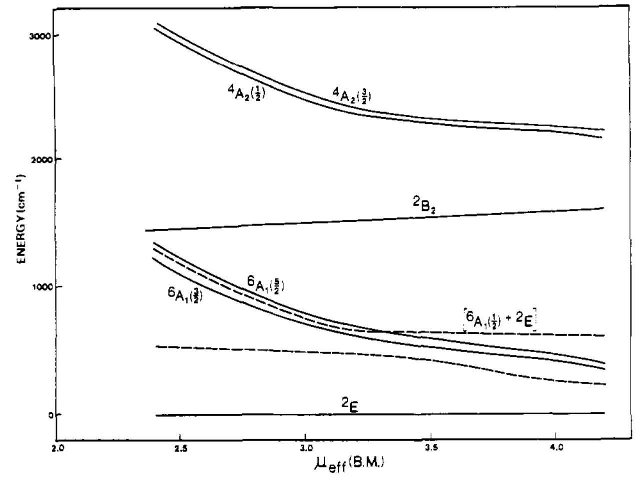

Figure 5. Ordering of the low-lying energy levels of the Fe(OEP)X$_2$ClO$_4$ derivatives vs. their magnetic moments, at 320 K. The solid lines refer to levels that are predominantly single component states while the dashed lines represent a varying composition of $^6A_1$ ($^1/_2$) and ^2E (see text).

It is interesting to see that the very different magnetic properties of the present iron compounds can arise from an energy level diagram which is qualitatively, remarkably similar for all the derivatives. The key apparently lies in the composition of the first excited state and probably to a lesser degree its energy relative to the ground state. This of course is only possible in the complicated spin-mixed region. It is to be noted that, although the first excited state is largely $^6A_1$ ($^1/_2$), the calculated limiting magnetic moment for the 3-chloropyridine derivative at, e.g., 400 K is 4.4 μ_B and at 500 K it is still only 4.5 μ_B, in nice agreement with the trend in Figure 2. A roughly constant magnetic moment of between 4.0 and 4.5 μ_B is then not *necessarily* indicative of, in this case, a spin quartet first excited state. Another interesting observation, although not obvious unless the eigenvectors are inspected in detail, is the effect of the magnetic-field mixing which is included in the diagonalization of the energy matrix. In the $z(\|)$ direction all the magnetic-field matrix elements are diagonal, so there is no mixing and each Kramers doublet contains mutually exclusive components. In the $x,y(\perp)$ direction all the matrix elements are off diagonal resulting in the two components of each Kramers doublet containing the same proportion of *all* the basis states contributing to the particular level.

Three further points are of interest. First, the ESR of all the derivatives (20 K)[13] show a strong absorption at $g \simeq 0.55$

---

[15] Hall, G. R.; Hendrickson, D. N. *Inorg. Chem.* **1976**, *15*, 607.

and a weaker one at $g \simeq 4.0$. These cannot be easily predicted by using a pure $^2T_{2g}$ ground state but are exactly the values predicted from the present spin-mixed model. However there are other smaller absorptions ($g = 1.5$–6) which may be due to impurities. Second, the Mössbauer data[13] of $Fe(OEP)(py)_2ClO_4$ definitely shows the presence of two sets of spectra at 300 K, the $S = {}^5/_2$ or $S = {}^3/_2$ spectra all but disappearing by 77 K. Whether this is compatible with the energy level diagram in Figure 5 or whether it indicates the exclusive presence of two different individual species is an open question although both could be compatible with the present model. Finally the solid-state magnetic data[3b] are exactly the same for the predominately low-spin derivatives in Figure 2. The higher magnetic moment derivatives are a little different in the solid state (limiting magnetic moment of 4.9 μ_B at 300 K) which is again to be expected in the present model. In the low-spin cases the sensitive region of parameter space has been passed so small changes in the metal environment will have little or no effect on the observed properties. However in the high-spin region the iron atom is in a sensitive situation where very small changes in environment can and indeed would be expected to produce significant changes in the magnetic moment. Calculations suggest that a change in C' of only 50 cm^{-1} is enough to raise the magnetic moment to 4.9 μ_B. Indeed the model can predict a $S = {}^1/_2$–$S = {}^5/_2$ equilibrium with magnetic moments up to 5.8 μ_B and down to 2.2 μ_B along with *limiting* values of 4.5 μ_B for the solution 3-chloropyridine derivative.

Several recent articles have dealt with the interaction of the three possible spin states in iron(III) complexes. Sinn et al.[16] discuss the possibility of an $S = {}^3/_2$ ground state for several tris(morpholinocarbodithioato-*S,S'*)iron(III) solvates. The presence of H_2O or $CHCl_3$ in the lattice appears to produce a low-lying $S = {}^3/_2$ state while CH_2Cl_2 incorporated into the lattice produces a genuine $S = {}^3/_2$ ground state. It follows that a relatively low-lying $S = {}^3/_2$ state will exist for all of the iron(III) dithiocarbamates, and so it is concluded that strong spin–orbit coupling will exist between the three states. This may help to explain why Hall and Hendrickson[15] were not able to account exactly for several of the g values in the $Fe(dtc)_3$ systems as they only took into account the pure $^6A_1$ and ^2T_g states. Dolphin et al.[2] have presented evidence that the ground state in $Fe(OEP)ClO_4$ is also a quantum mechanical admixture of spin quartet and spin sextet states with the quartet lying lower. Reed et al.[17] have also postulated the presence of an $S = {}^3/_2$–$S = {}^5/_2$ spin equilibrium in perchloro(mesotetraphenylporphinato)iron(III). However the evidence was interpreted qualitatively by using Maltempo's results[1] which only considered quantum mechanical mixing between the $S = {}^3/_2$ and $S = {}^5/_2$ states. The present calculations involve the *three* different spin states, and as pointed out above it is possible to obtain magnetic moments which behave as if the $S = {}^3/_2$ state were the predominant compoment of the ground state whereas in fact the equilibrium is actually between $S = {}^1/_2$ and $S = {}^5/_2$ with the $S = {}^3/_2$ state some thousands of cm^{-1} higher in energy (Figure 5).

The Isotropic NMR Shifts

The observed isotropic shift is a combination of pseudocontact and contact contributions. In expression 1 for the

$$\frac{\Delta H}{H} = \frac{1}{3R^3}(1 - 3\cos^2\theta)(K_\parallel - K_\perp) \qquad (1)$$

pseudocontact shift (usual symbols) it is often quite unrealistic to calculate $(K_\parallel - K_\perp)$ by using g values, especially for these compounds where a large number of interacting spin levels all contribute in different ways to the susceptibility tensor. In the present situation we are able to use $(K_\parallel - K_\perp)$ from the previous section (calculated by using $\partial E/\partial H$ and the field strength of the NMR spectrometer), and with known geometrical factors the pseudocontact shift can then be calculated directly. Two assumptions have been made in the use of eq 1. The susceptibility tensor has been assumed to possess axial symmetry[18] and ligand contributions to the pseudocontact shift have been ignored.[19] However at this stage the extra effort involved is not warranted.

Table II. Some Representative Experimental and Theoretical NMR Isotropic Shifts for Several $Fe(OEP)X_2ClO_4$ Derivatives

T/K	$(K_\parallel - K_\perp)$/ 10^{-6} cm^3 mol^{-1} [a]	pcon/ ppm[a]	con/ ppm[a,b]	total shift/ ppm[a]	obsd shift/ ppm[c]
(1) β-Pyridine Protons: $\theta^d = -0.11 \times 10^{23}$ cm^{-3}					
(i) $Fe(OEP)(3\text{-Cl-py})_2ClO_4$					
320	742	−4.5	−28.2	−32.7	
260	2461	−15.0	−8.9	−24.0	
200	5215	−31.8	12.31	−19.4	−19.0
(ii) $Fe(OEP)(4\text{-ac-py})_2ClO_4$					
320	1327	−7.5	−16.3	−23.9	−24.2
260	2790	−17.0	0	−17.0	−15.7
200	5116	−29.3	12.4	−16.9	−17.5
(iii) $Fe(OEP)(3\text{-ac-py})_2ClO_4$					
320	1518	−9.2	−13.4	−22.3	−22.9
260	3105	−18.9	2.9	−16.0	−15.5
200	5138	−31.3	14.3	−17.0	−18.5
(iv) $Fe(OEP)(py)_2ClO_4$					
320	2267	−13.8	−5.3	−19.1	−19.7
260	3761	−22.9	9.6	−13.2	−13.6
200	5556	−33.8	16.4	−17.4	−18.0
(2) α-Pyridine Protons: $\theta^d = -0.204 \times 10^{23}$ cm^{-3}					
(i) $Fe(OEP)(py)_2ClO_4$					
260	3761	−42.5	50.6	8.1	6.5
200	5556	−62.7	73.0	10.3	10.7
(ii) $Fe(OEP)(3\text{-ac-py})_2ClO_4$					
260	3105	−35.0	41.0	6.0	6.0
200	5138	−58.0	67.2	9.2	10.0

[a] Calculated by using the parameters from Table I. [b] The calculated hyperfine coupling constants are listed in Table III. [c] Taken from ref 4. [d] The geometric factor $(1 - 3\cos^2\theta)/r^3$ (from ref 4).

The contact contribution to the isotropic shift is given by eq 2 (usual symbols) where we have allowed the hyperfine

$$\frac{\Delta H}{H} = \frac{\sum A_i\langle S_{iz}\rangle}{\gamma_N/2\pi} \qquad (2)$$

coupling constant A_i associated with each state i to be different. In principle separate coupling constants could be assigned to each of the spin quartet and doublet states and to the sextet state, but for minimization of the number of unknown parameters only three were used $A_{^6A}$, $A_{^4A,^4E}$, and $A_{^2B,^2E}$. In practice the calculation of $\sum A_i\langle S_{iz}\rangle$ is performed by an extra subroutine (NMR) in the general susceptibility calculation.[10]

---

(16) Butcher, R. J.; Ferraro, J. R.; Sinn, E. *J. Chem. Soc., Chem. Commun.* **1976**, 910.

(17) Reed, C. A.; Mashiko, T.; Bently, S. P.; Kastner, M. E.; Scheidt, W. R.; Spartalian, K.; Lang, G. *J. Am. Chem. Soc.* **1979**, *101*, 1948.

(18) This may not be valid as low-spin d^5 systems are notoriously low in symmetry; e.g., g_x, g_y, and g_z in several porphyrin and hemin systems [Horrocks, W. De W.; Greenberg, E. S. *Mol. Phys.* **1974**, *27*, 993] and even the orbitally nondegenerate $^4A_2$ ground states of $Fe(dtc)_2X$ (X = Cl, Br, or I) show quite marked rhombic character [Ganguli, P.; Marathe, V. R.; Mitra, S.; Martin, R. L. *Chem. Phys. Lett.* **1974**, *26*, 529].

(19) For low-spin iron(III) compounds this could be a serious omission: Kurland, R. J.; McGarvey, R. B. *J. Magn. Reson.* **1970**, 2, 286.

Table III. Some Representative Calculated Hyperfine Coupling Constants ($\times 10^5$ Hz) for Several $Fe(OEP)X_2ClO_4$ Derivatives

protons	derivative	coupling const ^6A	$^4E, {}^4A$	$^2E, {}^2B$
β-pyridine	3-chloropyridine	3.5	0.5	−1.8
	4-acetylpyridine	3.4	0.4	−2.2
	3-acetylpyridine	3.4	0.5	−2.0
	pyridine	4.5	0.7	−1.5
b_{16}	3-chloropyridine	2.4	2.4	0.8
	4-acetylpyridine	2.2	2.2	0.6
	3-acetylpyridine	2.8	2.4	0.4
	pyridine	3.2	2.6	0.9
	N-methylimidazole	3.5	2.6	0.8
α-pyridine	pyridine	6.0	−1.0	−5.7
	3-acetylpyridine	3.0	−1.0	−6.0

Our technique in the present series of $Fe^{III}(OEP)$ complexes is to use the principal susceptibilities which gave rise to the average magnetic moments described in the previous section, together with the known geometrical factors, to calculate the pseudocontact shifts. With the differing amounts of high-, low-, and intermediate-spin contributions in the spin-mixed region the anisotropy in susceptibility as a function of temperature can vary greatly and is often crucial in accounting quantitatively for the overall shifts. If the observed isotropic shifts (Table II) can be represented by the sum of (1) and (2), then the only unknowns are the three A_i values. Perhaps surprisingly it was not difficult to find apparent best fit values for each of them, the temperature variation of the observed shift vs. T being the key factor in this analysis.

With temperature-independent ligand-field parameters several of the unusual isotropic shifts could not be reproduced by using the above procedure, and a qualitative examination indicated that this problem nearly exactly paralleled the difficulties encountered with the magnetic moments. Temperature-dependent ligand-field values make a significant difference to the calculated shifts and allow a ready explanation of most of the experimental proton NMR data. It must be pointed out though that this is only necessary for certain resonances (e.g., the β-pyridine protons of $Fe^{III}(OEP)(4\text{-ac-py})_2ClO_4$ (ac-py = acetylpyridine). In other cases the three coupling constants may provide enough flexibility to absorb the temperature-varying ligand field. The results from the β-pyridine proton shifts are shown in Table II. The same analyses were made for the b_{16} and α-pyridine protons; the resulting calculated hyperfine coupling constants are collected together in Table III. The particular example of the β-pyridine proton resonance in $Fe(OEP)(3\text{-ac-py})_2ClO_4$ is shown graphically in Figure 6. The effect of the temperature-dependent ligand-field parameters on the calculated isotropic shifts and the need for them is certainly well illustrated.

The calculated shifts of the α-pyridine protons in Table II are to be particularly noted. Although the observed isotropic shift is rather small, the geometrical factor coupled with the large calculated anisotropy in susceptibility makes the pseudocontact contribution quite large and opposite in sign to the observed shift. Consequently the contact part of the shift has to be large and to be of opposite sign, and so the experimental shift and its temperature variation are a delicate balance between two large calculated values. In fact this applied to most of the resonances which were observed and fitted to the above model.

Although the derived coupling constants may not be unique, several qualitative observations can be made. For example dissimilar coupling constants for the same resonance position may be expected in differently substituted adducts (different donor properties, etc.), but these effects must be relatively small because the values in Table III suggest that, in the main, the changing ligand field can accommodate most of the varying shifts. Taking average values of the coupling constants and neglecting the quartet spin states, because they contribute little to the observed properties, we find the following values ($\times 10^5$ Hz) for the various positions defined in Figure 1.

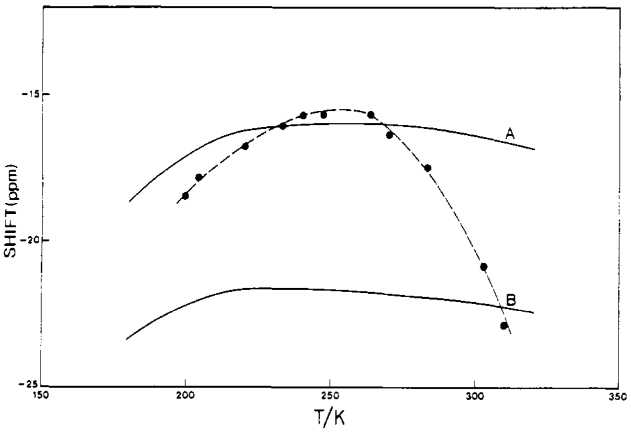

Figure 6. Temperature-dependent isotropic shifts of the β-pyridine proton resonance (●) in $Fe(OEP)(4\text{-ac-py})_2ClO_4$ and two representative descriptions: curve A with Δ_{Oh} = 31 970 and C' = 4400 cm^{-1}, respectively, and curve B with Δ_{Oh} = 32 000 and C' = 4380 cm^{-1}, respectively. Both have been calculated with the same hyperfine coupling constants (see Table III).

	^6A	^2E		^6A	^2E
α	5	−6	a	1	1
β	4	−2	b	3	1
γ	~0	−1	c	~0	0.5

The porphyrin a, b, and c protons have rather small coupling constants, the c position being, predictably, very small. The rather smaller than perhaps expected values for the a position (compared with the b position) may well reflect the predicted nodes (Hückel molecular orbital calculations[20]) at the methene bridge carbons in the porphyrin $3e_g$ orbitals. Surprisingly there appears to be no alteration in the sign of the coupling constants around the α, β, and γ positions of the pyridine adduct, the values decreasing away from the metal ions as would be expected in a σ-delocalization mechanism. The different coupling constant signs for the $^6A_1$ and ^2E states arise because of their different orbital configurations. In the high-spin case this is $|e^2b_2{}^1a_1{}^1b_1{}^1\rangle$ in the low-spin case it is $|e^3b_2{}^2\rangle$ so that in the two cases different spins and spin directions can be and are delocalized.

Over and above all the complications discussed so far, there also remains the problem of possible conformational changes in solution when the temperature is altered. This influence on the magnetic properties of the metal ions has, in effect, been taken account of with the varying ligand-field parameters but could lead to extra variation in the contact and pseudocontact contributions to the isotropic shift. The possibly inequivalent adducts (with the iron atom out of the N_4 plane) could also lead to complications which may even contribute to the line broadening, making the resonances difficult to observe at the higher temperatures.

Conclusions

The electronic structures of the $Fe(OEP)X_2ClO_4$ derivatives are complicated although several points seem clear. First, all the possible ground states of the iron atom in D_4 symmetry ($^6A_1$, $^4A_2$, and ^2E) are all quite close in energy, and so spin–orbit coupling between all three must be included for a realistic description of the ground- and excited-state properties of the metal ion. This is probably the case in many iron(III) por-

---

(20) Longuet-Higgins, H. C.; Rector, C. W.; Platt, J. R. *J. Chem. Phys.* **1950**, *18*, 1174.

phyrin derivatives. Second, within the framework of ligand-field theory, it is only possible to explain the magnetic properties in terms of a ^2E ground state with a first excited state some 200–400 cm^{-1} away, composed of varying amounts of $^6A_1$ and $^2E_1$ character, *and* by varying the ligand-field parameters slightly with temperature. Whatever the true description of the ligand field or of the vibronic nature of these systems the end observation (in the phenomenological description) of temperature-dependent parameters is necessary. Although not very satisfying, this latter requirement may well be compatible with the known geometry of other metal porphyrin compounds. Third, with these calculated parameters the observed NMR isotropic shifts can at least be reproduced quantitatively although the derived coupling constants are probably not unique. This is because they depend so critically on very small changes in the ligand-field parameters and so on the calculated pseudocontact shifts which in turn contribute quite substantially to the experimental shift.

The relation between electronic structure and biological activity is of particular current interest with several groups of workers actively engaged in preparing new synthetic model complexes, and particularly iron porphyrin derivatives, with this in mind. Although it is not yet established whether the particular electronic state of the iron atom controls or activates the biological function, the reverse is certainly true in that many different natural and synthetic iron complexes of this nature exhibit wide-ranging magnetic properties concomitant with the three nearly equienergetic, interacting ground states.

Acknowledgment. Very profitable discussions with Professor R. L. Martin and Drs. K. S. Murray, H. A. O. Hill, and P. D. Skyte are acknowledged.

Registry No. Fe(OEP)(3-Cl-py)$_2$ClO$_4$, 71414-31-8; Fe(OEP)(4-ac-py)$_2$ClO$_4$, 75149-73-4; Fe(OEP)(3-ac-py)$_2$ClO$_4$, 75172-95-1; Fe(OEP)(py)$_2$ClO$_4$, 71414-34-1; Fe(OEP)(*N*-me-im)$_2$ClO$_4$, 71414-35-2.

Contribution from the Department of Chemistry,
University of Washington, Seattle, Washington 98195

Porphyrins. 41.[1] Phosphorus Mesoporphyrin and Phthalocyanine

MARTIN GOUTERMAN,* PHILLIP SAYER, ERIC SHANKLAND, and JUSTIN P. SMITH

Received April 9, 1980

It is shown that synthesis of phosphorus porphyrins occurs from a pyridine–PBr$_3$ intermediate, and an improved synthetic procedure is given for P(MesoDME)(OH)$_2^+$ (MesoDME = mesoporphyrin dimethyl ester). The ^{31}P NMR spectral peaks occur between $\delta = -183$ and -197, depending on the solvent. The two protons of P(MesoDME)(OH)$_2^+$ can be titrated with p$K_{a1} = 9.53$ and p$K_{a2} = 12.20$, values obtained by monitoring the optical spectrum over the pH range 8–13 and the wavelength range 515–600 nm. Qualitatively the Q(0,0) or α band shifts from 583 nm at pH 7 to 561 nm at pH 13.3. This hypsochromic shift is attributed to back-bonding between the filled O(p$_x$,p$_y$) and the empty e$_g(\pi^*)$ orbitals. The fluorescence lifetime decreases with increased pH: 4.1 (pH 7), 3.1 (pH 10), 2.6 ns (pH 13). A stable phosphorus phthalocyanine complex, P^{III}(Pc), can be made. It has a sharp Soret band at 442 nm. Its unusual visible spectrum is attributed to the four-orbital transitions a$_{1u}(\pi)$, a$_{2u}$(3p$_z$) → e$_g(\pi^*)$. A strong red fluorescence at 660 nm has a lifetime of 3.0 ns. There is also evidence for a P^V(Pc) species with a visible absorption like that of Zn(Pc) but with no fluorescence.

Introduction

Over the past 15 years considerable research has gone into the preparation of porphyrin complexes with various metals, with the result that porphyrin complexes are known with nearly every metal and semimetal in the periodic table.[2-4] One of the last type of complexes reported is those of phosphorus.[5,6] Since the initial report from our laboratory,[5] we have carried out further studies of phosphorus porphyrins. Our interest arises because phosphorus is the lightest atom forming a metalloporphyrin where the "metal" shows two oxidation states, in this case P^{III} and P^V; hence ab initio studies of the two oxidation states should prove easier than for transition-metal porphyrins, which contain d electrons. A second interest arises because of the possible biological use of phosphorylated porphyrin, since "demetalation" produces harmless phosphate ions rather than toxic metals.

In this paper we report the results of further investigations of these species: (1) an improved synthetic method that suggests that "metalation" occurs from a reactive pyridine–PBr$_3$ intermediate; (2) the acid–base properties of phosphorylated mesoporphyrin; (3) preliminary studies of the ^{31}P NMR spectra of phosphorylated porphyrins; (4) the synthesis of phosphorus phthalocyanine, which shows a fluorescent P^{III}(Pc) species and a nonfluorescent P^V(Pc) species.

Synthesis of Phosphorus Mesoporphyrin

The first reported synthesis was of the phosphorus octaethylporphyrin (OEP) complex; it proceeded in two steps (eq 1 and 2). Step 1 required 30 min in pyridine at 80–90 °C,

$$\mathrm{H_2(OEP) + PCl_3 \rightarrow P^{III}(OEP)^+Cl^- + 2HCl} \qquad (1)$$

$$\mathrm{P^{III}(OEP)^+Cl^- + H_2O + {}^1/_2O_2 \rightarrow P^V(OEP)(OH)_2{}^+Cl^-} \qquad (2)$$

with a mole ratio of PCl$_3$ to H$_2$(OEP) of 120:1. We were unable to carry out (1) in any solvent but pyridine. In particular it failed to go in amines, quinoline, or 2-picoline. Step 2 was presumed due to the presence of air and water.[5] In practice the oxidation step often failed, with the resulting re-formation of the free base H$_2$(OEP). Overall yields for P^V(OEP)(OH)$_2^+$ were never better than 30% and often were very poor. The second reported synthesis was of the P^V tetraphenylporphyrin (TPP) complex.[6] The reaction was carried out in pyridine with POCl$_3$, requiring 24 h at reflux temperature with a mole ratio of POCl$_3$ to H$_2$(TPP) of ~60:1.

In trying to improve the synthesis, we found that PBr$_3$ was better than PCl$_3$, and PI$_3$ gave no reaction. The following pieces of evidence show that PBr$_3$ forms a new, highly reactive species in pyridine. (1) On addition of PBr$_3$ to pyridine, the solution turns a bright, straw yellow color. (2) The PBr$_3$–pyridine solution reacts far more violently with paper than does either neat PBr$_3$ or pyridine. (3) Both neat ^{31}PBr$_3$ and ^{31}PBr$_3$ in CH$_2$Cl$_2$ show a structured line at $\delta = 228$.[7] In contrast,

---

(1) Part 40: Spellane, P. J.; Gouterman, M.; Antipas, A.; Kim, S.; Liu, Y. C. *Inorg. Chem.* **1980**, *19*, 386.
(2) Ostfeld, D.; Tsutsui, M. *Acc. Chem. Res.* **1974**, *7*, 52.
(3) Buchler, J. W. "The Porphyrins"; Dolphin, D., Ed.; Academic Press: New York, 1979; Vol. 1, Chapter 10, p 390.
(4) Gouterman, M. Reference 3, Vol. III, Chapter 1, p 1.
(5) Sayer, P.; Gouterman, M.; Connell, C. R. *J. Am. Chem. Soc.* **1977**, *99*, 1082.
(6) Tsutsui, M.; Carrano, C. J. *J. Coord. Chem.* **1977**, *7*, 79.